AGU PUBLICATIONS

Geophysical Research Letters

RESEARCH LETTER
10.1002/2017GL074457

**Key Points:**
- At the onset of the Last Interglacial, $\delta^{18}O$ of *Globorotalia inflata* remains close to glacial values for ~7 kyr
- High $\delta^{18}O$ at the onset of the Last Interglacial can be explained by the existence of a colder and/or saltier South Atlantic thermocline
- A colder thermocline may have resulted from the North Atlantic heat piracy, following the resumption of deepwater convection from ~129 ka

**Correspondence to:**
A. L. S. Albuquerque,
ana_albuquerque@id.uff.br

**Citation:**
Santos, T. P., Lessa, D. O., Venancio, I. M., Chiessi, C. M., Mulitza, S., Kuhnert, H., & Albuquerque, A. L. S. (2017). The impact of the AMOC resumption in the western South Atlantic thermocline at the onset of the Last Interglacial. *Geophysical Research Letters*, *44*. https://doi.org/10.1002/2017GL074457

Received 5 JUN 2017
Accepted 1 NOV 2017
Accepted article online 6 NOV 2017



# The Impact of the AMOC Resumption in the Western South Atlantic Thermocline at the Onset of the Last Interglacial

**Thiago P. Santos[1], Douglas O. Lessa[1], Igor M. Venancio[2,3], Cristiano M. Chiessi[4], Stefan Mulitza[2], Henning Kuhnert[2], and Ana Luiza S. Albuquerque[1]**

[1]Programa de Geociências (Geoquímica), Universidade Federal Fluminense, Niterói, Brazil, [2]MARUM-Center for Marine Environmental Sciences, University of Bremen, Bremen, Germany, [3]Center for Weather Forecasting and Climate Studies (CPTEC), National Institute for Space Research (INPE), Cachoeira Paulista, Brazil, [4]Escola de Artes, Ciências e Humanidades, Universidade de São Paulo, São Paulo, Brazil

**Abstract** After glacial terminations, large amounts of heat and salt were transferred from low to high latitudes, which is a crucial phenomenon for the reestablishment of the Atlantic Meridional Overturning Circulation (AMOC). However, how different glacial terminations evolved in the (sub)tropics is still poorly documented. Here we use foraminifera oxygen ($\delta^{18}O$) and carbon ($\delta^{13}C$) stable isotopes to show that the North Atlantic heat piracy, following the AMOC resumption at the early Last Interglacial, affected the thermocline $\delta^{18}O$ levels of the subtropical western South Atlantic. Because of the cooling imposed by this process, glacial $\delta^{18}O$ persisted in the thermocline for ~7 kyr after the onset of the Last Interglacial, dampening the effect of sea level rise usually imprinted on foraminifera $\delta^{18}O$ during terminations. Faunal composition and $\delta^{13}C$ also suggest the existence of a colder and thicker South Atlantic Central Water coeval with the AMOC recovery. This process apparently did not occur during the last deglaciation.

**Plain Language Summary** Glacial terminations are periods of fast ice sheet disintegration, elevation of global temperatures, and release of carbon dioxide from the deep ocean to the atmosphere. These conditions turn such intervals well situated to the study of global climate changes. The warming of high latitudes is supported by the transfer of heat and salt from low latitudes. However, the documentation of how glacial terminations occurred in low-latitude oceans are still poorly documented. In this study we show through oxygen isotopes of planktonic foraminifera that thermocline waters from the Brazilian margin may have worked as a source of hydrostatic instability to return the meridional circulation to its interglacial mode. The impact of this process may have produced a colder South Atlantic thermocline during the transition to the Last Interglacial (130 kyr ago).

## 1. Introduction

The "sawtooth"-shaped glacial-interglacial cycles shown by several benthic $\delta^{18}O$ records reflect long periods of ice growth followed by rapid deglaciations defined as terminations (Raymo, 1997). Several studies support a difference in the sequence of events associated with Termination I (TI, the last deglaciation) and Termination II (TII, the penultimate deglaciation) (Martrat et al., 2014; Masson-Delmotte et al., 2010; Stoner et al., 1995). Across TI, increased Atlantic Meridional Overturning Circulation (AMOC) was postulated for the Bølling-Allerød period, followed by the Younger Dryas, which promoted an abrupt return to glacial conditions in high latitudes of Northern Hemisphere (McManus et al., 2004; Ritz et al., 2013). Otherwise, there is no clear evidence of a Younger Dryas-like event during TII, and the AMOC strengthening only occurred close to the very end of this transition (Lototskaya & Ganssen, 1999).

Carlson (2008) argues that the contrasting relative timings of deglacial AMOC resumption may be a consequence of greater boreal summer insolation during TII, leading to faster ice sheet decay and meltwater input that would have suppressed AMOC throughout this transition. Differences in maximum summer insolation at high southern latitudes may also explain the distinct timing of the events that characterize these glacial terminations (Broecker & Henderson, 1998). Irrespective of the dynamics of each glacial termination, at the end of these events, extensive amounts of salt and heat were mobilized from tropical/subtropical oceans (e.g., Schmidt et al., 2004), deepening the overturning cell and warming atmospheric temperatures at high latitudes.

Nonetheless, the evolution of different glacial terminations at low latitudes is poorly known. In this study, we use foraminifera oxygen ($\delta^{18}O$) and carbon ($\delta^{13}C$) stable isotopes to document the last two glacial-interglacial

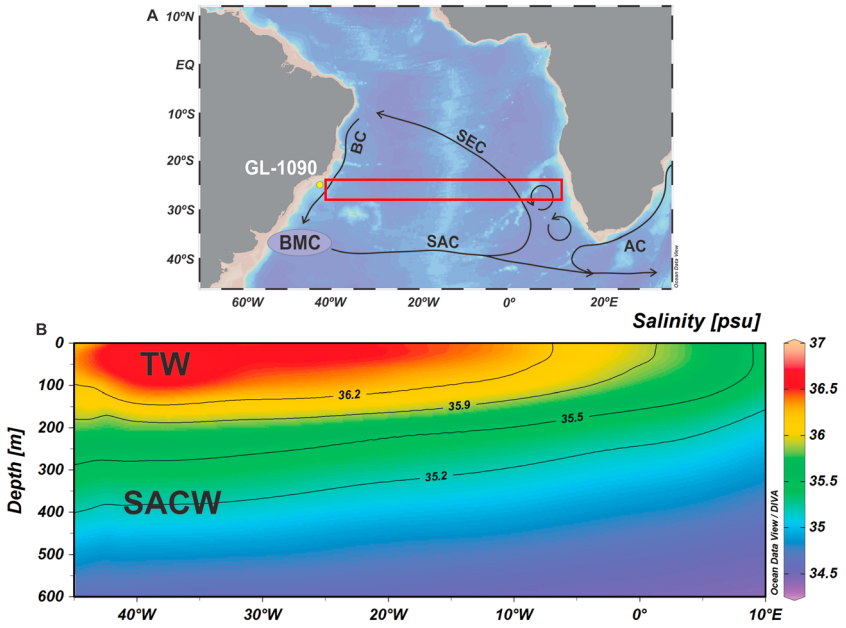


**Figure 1.** Position of core GL-1090 (Santos Basin, 24.92°S, 42.51°W, 2225 m water depth, 1914 cm long; this study). (a) Schematic representation of the main currents of the South Atlantic subtropical gyre (SEC, South Equatorial Current; BC, Brazil Current; SAC, South Atlantic Current), together with the Agulhas Current (AC) and the Brazil-Malvinas Confluence (BMC) (Stramma & England, 1999). (b) Upper South Atlantic salinity (Zweng et al., 2013) integrated across the area highlighted by the red rectangle on Figure 1a (TW, Tropical Water; SACW, South Atlantic Central Water). This figure was partly created with Ocean Data View (Schlitzer, 2003).

transitions in the subtropical western South Atlantic. Whereas TI displays nearly simultaneous surface, thermocline and middepth $\delta^{18}O$ shifts, a different pattern emerges for TII. Our data show that the thermocline $\delta^{18}O$ remained at glacial levels for ~7 kyr after the onset of the Last Interglacial. Only during late marine isotope stage (MIS) 5e the thermocline $\delta^{18}O$ shifted toward interglacial values. These findings imply that rapid freshwater input from disintegrating ice sheets, which usually controls foraminifera $\delta^{18}O$ during terminations, was damped by another forcing able to produce a glacial-like pattern over a large part of the Last Interglacial. We propose that a strong cooling in the thermocline of the subtropical western South Atlantic following the AMOC resumption at the beginning of the Last Interglacial substantially influenced $\delta^{18}O$ and masked the effect of sea level rise. Salt waters sourced from the Indian Ocean via Agulhas Leakage may also have contributed for this remarkable isotopic configuration.

## 2. Study Site

Marine sediment core GL-1090 was collected by Petrobras within the Santos Basin (western South Atlantic, 24.92°S, 42.51°W, 2225 m water depth, 1914 cm long) (Figure 1a). The southward flowing Brazil Current dominates the upper circulation in this region (Figure 1a). At the surface, the high incoming solar radiation and excess evaporation that characterize the tropical South Atlantic contribute to form the warm ($>$ 20°C) and saline ($>$ 36.2) Tropical Water (Stramma & England, 1999). In the thermocline (~100–600 m), the Brazil Current transports the colder (14–16°C) and fresher (34.5–36.2) South Atlantic Central Water (SACW) (Peterson & Stramma, 1991) (Figure 1b). Beyond temperature and salinity, Tropical Water and SACW can also be distinguished by their $\delta^{13}C$ of dissolved inorganic carbon, in which Tropical Water $\delta^{13}C_{DIC}$ = 1.74 ± 0.24 and SACW $\delta^{13}C_{DIC}$ = 1.30 ± 0.22 (Venancio et al., 2014). The $\delta^{13}C_{DIC}$ offset between Tropical Water and SACW reflects the higher nutrient content of SACW, as $\delta^{13}C_{DIC}$ decreases along with increasing nutrient concentration (Broecker & Maier-Reimer, 1992). SACW ventilates the South Atlantic thermocline, and two sites are involved in its formation. Around 38°S, the Brazil Current collides with the northward flowing Malvinas Current, producing the Brazil-Malvinas Confluence (Figure 1a). In this region and locations between the Argentine basin and the mid-Atlantic ridge, thermocline water is generated by air-sea interaction (Garzoli & Matano, 2011). SACW is also sourced from Indian Ocean Central Water and brought into the South Atlantic by Agulhas eddies in the upper 1000 m of the water column (Richardson, 2007; Tomczak & Godfrey, 1994). Thus, the Brazil-Malvinas Confluence (and adjacent areas) and Agulhas Leakage represent the major areas

of formation of SACW and are crucial for ventilating the South Atlantic thermocline (Gordon, 1981). At the study site, the sediment surface is bathed by the upper portion of North Atlantic Deep Water that originates from the northern North Atlantic (Stramma & England, 1999).

## 3. Material and Methods

The 1914 cm of core GL-1090 cover the last 185 ka. The age model was obtained through a combination of calibrated AMS $^{14}$C ages and benthic foraminifera $\delta^{18}$O tie points aligned to two reference curves (Govin et al., 2014; Lisiecki & Raymo, 2005). Age modeling was based on the software Bacon v.2.2, which reconstructs Bayesian accumulation histories for sedimentary deposits (Blaauw & Christeny, 2011). Details regarding age model and sedimentation rates are provided by Santos et al. (2017). Here we focus on the intervals of the penultimate (140–116 ka) and last (30–6 ka) glacial-interglacial transitions. In order to monitor surface, thermocline and middepth $\delta^{18}$O evolution through TII and TI, we measured the oxygen isotopic composition of three different foraminifera species. We used the planktonic species *Globigerinoides ruber* (250–300 μm, white variety) to profile the surface mixed layer and the benthic species *Cibicides wuellerstorfi* (250–300 μm) for middepths (~2200 m). $\delta^{18}$O data of *G. ruber*, and *C. wuellerstorfi* were previously published in Santos et al. (2017).

We selected the species *Globorotalia inflata* for the thermocline since it shows an apparent calcification depth of 350–400 m in the South Atlantic (Groeneveld & Chiessi, 2011). We also present the carbon isotope composition ($\delta^{13}$C) of the same species. Previous studies have applied the geochemical composition of *G. inflata* to reconstruct past thermocline conditions, the migration of midlatitude oceanic fronts, and the carbon isotopic composition of the SACW (Campos et al., 2017; Chiessi et al., 2008; Voigt et al., 2015). For every sample, between 5 and 10 shells of *G. inflata* from the 250–300 μm size fraction were handpicked under a stereomicroscope. Analyses were performed at MARUM-Center for Marine Environmental Sciences, University of Bremen, Germany, using a Finnigan MAT252 gas isotope ratio mass spectrometer attached to a Kiel III automated carbonate preparation device. Data were calibrated against an in-house standard (Solnhofen limestone). The results are reported in per mil (‰, parts per thousand) versus Vienna Peedee belemnite (VPDB). The standard deviation based on replicate measurements of the in-house standard was 0.06 and 0.03‰ for $\delta^{18}$O and $\delta^{13}$C, respectively.

## 4. Results

Figure 2 presents the evolution of surface (*G. ruber*), thermocline (*G. inflata*), and middepth (*C. wuellerstorfi*) $\delta^{18}$O across TI (Figures 2a–2c) and TII (Figures 2d–2f). During TII (MIS 6/MIS 5e transition), surface and middepth $\delta^{18}$O markedly shifted at 130 ka, decreasing by 1.5‰ and 2.0‰, respectively (Figures 2d and 2f). However, at 130 ka, no noticeable change occurred in *G. inflata* $\delta^{18}$O (Figure 2e). Only in late MIS 5e did *G. inflata* $\delta^{18}$O finally shift to the low values characteristic of interglacial climate, with an amplitude of ~1.0‰ (Figure 2e). During TI (MIS 2/MIS 1 transition), $\delta^{18}$O of all three species shifted nearly simultaneously, with amplitudes of approximately 1.3‰, 0.8‰ and 1.5‰ for the surface, thermocline, and middepth ocean, respectively (Figures 2a–2c). Changes during TI were more sluggish than during TII; whereas surface, thermocline, and middepth $\delta^{18}$O took ~11 kyr to reach interglacial levels in TI, changes during TII occurred within ~2 kyr at the surface and thermocline levels and within ~5 kyr for middepth waters (Figure 2).

Figure 3 presents the evolution of *G. inflata* $\delta^{13}$C across TI (Figure 3a) and TII (Figure 3b). In early MIS 2, *G. inflata* $\delta^{13}$C showed values around 1.0‰ that lasted until the Last Glacial Maximum (LGM). During TI occurred the lowest values of the last glacial cycle of ~0.6‰ between 18 and 15 ka. In the transition to the Holocene, *G. inflata* $\delta^{13}$C returned to the values found during early MIS 2 (Figure 3a). Penultimate glacial cycle was generally characterized by $\delta^{13}$C ~0.3‰ lower than those of the last glacial cycle (Figure 3b). At the end of penultimate glacial, *G. inflata* $\delta^{13}$C exhibited an increase toward TII, reaching its maximum values of ~0.9‰ between 135 and 130 ka. The transition to the Last Interglacial is marked by a decrease in *G. inflata* $\delta^{13}$C, when values as low as 0.4‰ were recorded until ~123 ka. After this age, *G. inflata* $\delta^{13}$C returned to the high values prevalent during TII (Figure 3b).

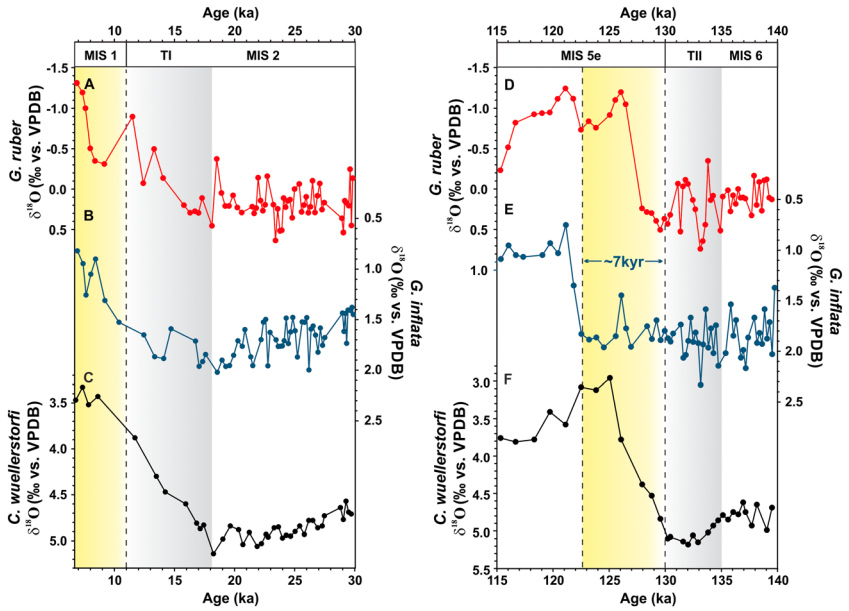


**Figure 2.** Evolution of surface, thermocline, and middepth $\delta^{18}O$ of the subtropical western South Atlantic throughout Termination I (TI, Figures 2a–2c) and Termination II (TII, Figures 2d–2f). (a, d) *Globigerinoides ruber* $\delta^{18}O$ (Santos et al., 2017). (b, e) *Globorotalia inflata* $\delta^{18}O$ (this study). (c, f) *Cibicides wuellerstorfi* $\delta^{18}O$ (Santos et al., 2017). Dashed lines mark the beginning of the current and Last Interglacial climate. Note that *G. inflata* $\delta^{18}O$ remained mostly unchanged until ~123 ka in the case of the Last Interglacial (Figure 2e). Gray bars highlight TI and TII and yellow bars highlight interglacial intervals.

## 5. Discussion

The fact that *G. inflata* $\delta^{18}O$ continued in a "glacial" pattern (~1.8‰) at the onset of the Last Interglacial (Figure 4c), while *G. ruber* $\delta^{18}O$ shifted to low interglacial values (~ −1.0‰) (Figure 2d), resulted in a sharp $\Delta\delta^{18}O$ between *G. inflata* and *G. ruber*, indicative of a high upper ocean stratification in the Santos basin (Figure 4d). The onset of the Last Interglacial in this region also resides a shift toward a carbon isotope minimum in *G. inflata* $\delta^{13}C$ (Figure 4e). This $\delta^{13}C$ minimum likely reflects the breakdown of the water column stratification in the Southern Ocean at the end of penultimate glacial and renewed upwelling of low-$\delta^{13}C$ waters (Ziegler et al., 2013). The advection of these waters to the boundary of the Subtropical Front and their subsequent subduction spread a low-$\delta^{13}C$ signal into the South Atlantic thermocline (Campos et al., 2017; Ziegler et al., 2013). The change from high to low *G. inflata* $\delta^{13}C$ at the beginning of MIS 5e also suggests an intensified export of preformed nutrients to the thermocline, which likely accompanied a thickening of the SACW. The transition to the Last Interglacial is also marked by a noticeable increase in the relative abundance of planktonic foraminifera *Globigerina bulloides* (Lessa et al., 2017) (Figure 4f). *G. bulloides* is known for tracking high productivity conditions, mainly associated with seasonal upwelling (Peeters et al., 2002;

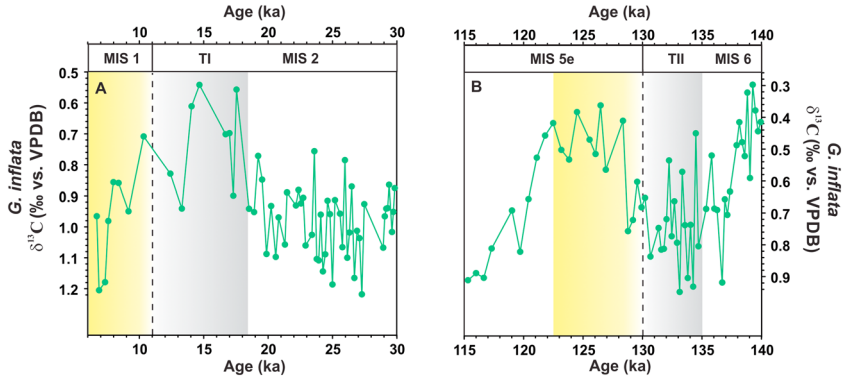


**Figure 3.** Evolution of thermocline $\delta^{13}C$ of the subtropical western South Atlantic throughout (a) Termination I (TI) and (b) Termination II (TII). *Globorotalia inflata* $\delta^{13}C$ (Figures 3a and 3b). Dashed lines mark the beginning of the current and Last Interglacial climate. Gray bars highlight TI and TII, and yellow bars highlight interglacial intervals.

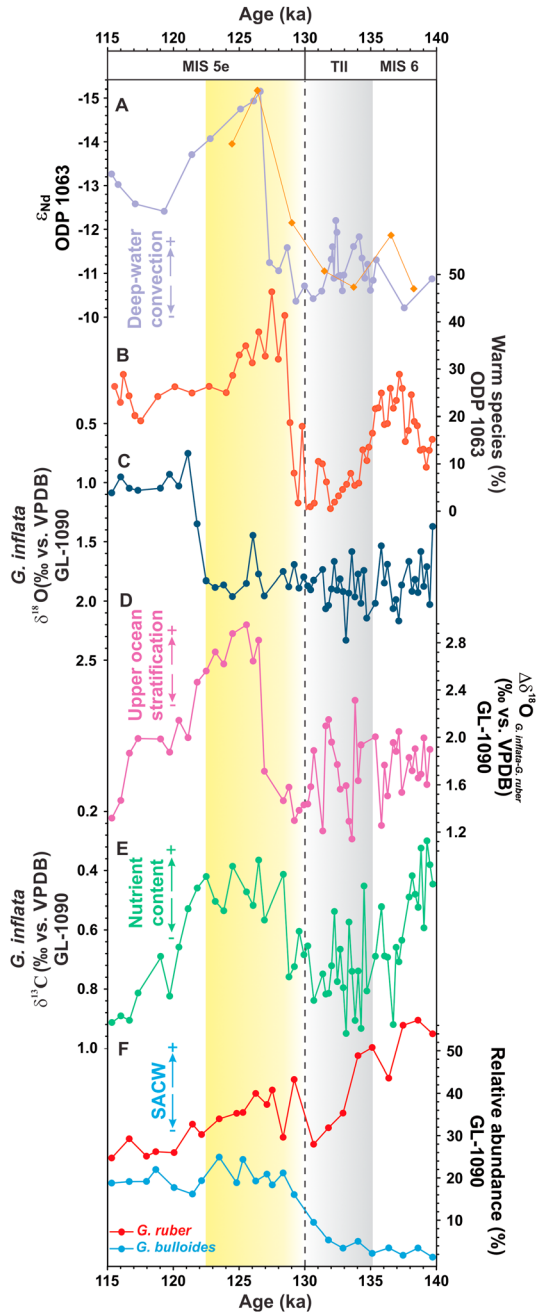


**Figure 4.** Configuration of the western South Atlantic thermocline (Santos Basin) during the return of deepwater convection at the onset of the Last Interglacial together with records from North Atlantic core ODP 1063 (Bermuda Rise). (a) $\varepsilon_{Nd}$ from Fe-Mn oxyhydroxide fraction of bulk sediment (purple circles) (Böhm et al., 2015) and $\varepsilon_{Nd}$ from fossil fish teeth and debris (orange diamonds) (Deaney et al., 2017) of ODP 1063. (b) Relative abundance of warm species (*Globigerinoides ruber* + *Globigerinoides sacculifer*) of ODP 1063 (Deaney et al., 2017). (c) *Globorotalia inflata* $\delta^{18}O$ (Santos basin, this study). (d) Upper ocean stratification estimated through $\Delta\delta^{18}O$ between *Globorotalia inflata* $\delta^{18}O$ and *Globigerinoides ruber* $\delta^{18}O$ of GL-1090 (Santos Basin, this study). (e) *Globorotalia inflata* $\delta^{13}C$ of GL-1090 (Santos Basin, this study). (f) Relative abundance (%) of *Globigerina bulloides* (light blue) and *Globigerinoides ruber* (red) of GL-1090 (Lessa et al., 2017). Dashed line marks the beginning of the Last Interglacial climate. Gray bar highlights TII, and yellow bar highlights part of the Last Interglacial.

Salgueiro et al., 2008; Tedesco et al., 2007). In the southeast Brazilian margin, a higher nutrient content in the SACW fueling the bottom of the mixed layer would favor the proliferation of *G. bulloides* in moments of SACW shoaling, but it would disrupt the optimal conditions for *Globigerinoides ruber* (Lessa et al., 2014, 2017; Portilho-Ramos et al., 2015). Thus, (1) high *G. inflata* $\delta^{18}O$, (2) a strong upper ocean stratification, (3) low *G. inflata* $\delta^{13}C$, and (4) the increase in the relative abundance of *G. bulloides* (and decrease in *G. ruber*) suggest that the thermocline of the western South Atlantic was marked by a thicker and likely colder SACW in the earlier stages of the Last Interglacial (Figures 4c–4f).

The early Last Interglacial also bears an abrupt AMOC reinvigoration. Recently, Deaney et al. (2017) proposed that the AMOC recovery following Heinrich stadial 11 was accomplished by a drastic deepening of the overturning cell in the NW Atlantic at ~129 ka. According to these authors, the long duration of Heinrich stadial 11 was related to the magnitude of the AMOC recovery (overshoot) at the beginning of MIS 5e and this was responsible for the larger $CO_2$ increase (by ~20 ppmv) of TII compared to TI. This overshoot would have been feasible by the rapid invasion of heat and salt accumulated in the tropical Atlantic during the AMOC collapse, which entered the NW Atlantic and induced hydrostatic instability. The AMOC overshoot, consequently, increases the North Atlantic heat piracy, cooling the low-latitude Atlantic (Seidov & Maslin, 2001). Hence, a longer AMOC weakening leads to a larger overshoot and heat piracy following the reinvigoration.

Our data show that thermocline waters from locations as far south as 24°S, and not only from the tropical Atlantic, as is commonly assumed based on the scenario of the last deglaciation (e.g., Rühlemann et al., 2004, Schmidt et al., 2012), may have been directly involved in this process. The thickening and cooling of the SACW estimated by our data correlate well with the occurrence of very unradiogenic neodymium isotopic values and the predominance of warm-water species of planktonic foraminifera in the Bermuda Rise (North Atlantic) (Figure 4) (Böhm et al., 2015; Deaney et al., 2017). This suggests that the expansion of the SACW and a better ventilated thermocline in the subtropical western South Atlantic accompanied the return of deepwater convection and the warmth in northern high latitudes (Figure 4). As a substantial part of the North Atlantic heat piracy occurred at earlier stages of MIS 5e (following the AMOC overshoot), the cooling in the South Atlantic thermocline imposed by this process from ~129 ka on could have reduced the temperature where *G. inflata* calcifies, contributing to delay the $\delta^{18}O$ transition until ~123 ka (Figures 2e and 4c).

In order to better evaluate the role of temperature change in thermocline $\delta^{18}O$ variability, we subtracted the ice volume effect considering the sea level reconstruction of Grant et al. (2012) and a glacial $\delta^{18}O$ increase of 0.008‰ $m^{-1}$ sea level lowering (Schrag et al., 2002). We verified that even subtracting the ice volume effect, *G. inflata* $\delta^{18}O$ remained ~1.0‰ higher between ~129 and 123 ka. During this interval, the offset between measured and corrected *G. inflata* $\delta^{18}O$ virtually disappears (Figure 5). The ~1.0‰ higher $\delta^{18}O$ in a time of decreasing influence of ice volume may have been caused by a cooling of 3–4°C, which is consistent with simulations of AMOC overshoot that produce a 3°C cooling in the thermocline of the western Atlantic (e.g., Gong et al., 2013). The longevity of the high $\delta^{18}O$ (and high $\Delta\delta^{18}O$) and low $\delta^{13}C$ signals corroborate that the

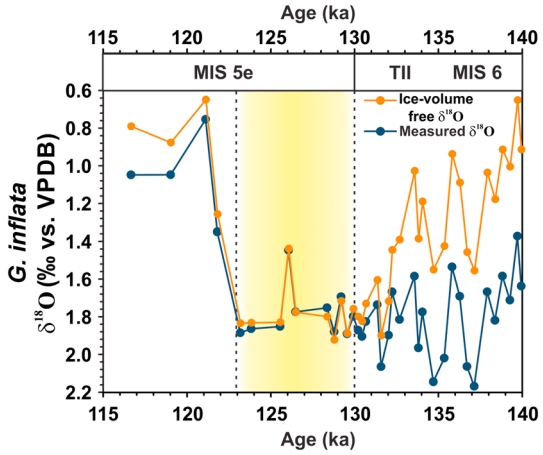


**Figure 5.** Measured (dark blue) and ice volume corrected (orange) *Globorotalia inflata* $\delta^{18}O$ during the penultimate glacial-interglacial transition. Ice volume correction takes into account the sea level reconstruction of Grant et al. (2012) and a glacial $\delta^{18}O$ enrichment of 0.008‰ $m^{-1}$ sea level (Schrag et al., 2002). Yellow bar highlights the interval of the Last Interglacial between ~129 and 123 ka, when high $\delta^{18}O$ values were still present in the thermocline of the Santos Basin, despite the reduced global ice volume influence.

expanded SACW may have experienced the impact of the heat piracy continuously between ~129 and 123 ka (Figures 4c–4e), as deepwater formation in the NE Atlantic may not have acquired its typical interglacial mode until ~124 ka (Deaney et al., 2017). The stabilization of the AMOC interglacial mode after ~124 ka may have reduced the intensity of the North Atlantic heat piracy and finally allowed the transition of *G. inflata* $\delta^{18}O$ to its low interglacial level (Figures 4c and 5). During the last deglaciation, minimum *G. inflata* $\delta^{13}C$ resembling that of the early Last Interglacial occurred along Heinrich stadial 1 (Figure 3a), but the thermocline $\delta^{18}O$ did not present a pattern decoupled from surface and middepth $\delta^{18}O$ (Figures 2a–2c). This may suggest that the North Atlantic heat piracy was not strong enough to influence the thermocline from latitudes so far south during TI. In this case, the modulation of ice volume/sea level adjustments over *G. inflata* shells dominated the oxygen isotope fractionation (Shackleton, 1987). This means that the intensity of the AMOC overshoot controls the degree to which the thermocline of the subtropical western South Atlantic will be affected.

Cold temperatures generated by the North Atlantic heat piracy may not be the only explanation for the pattern of *G. inflata* $\delta^{18}O$ during the TII/MIS 5e period. Based on ice volume-corrected seawater $\delta^{18}O$ (a proxy for salinity), Scussolini et al. (2015) described an increase of surface and thermocline salinity associated with the reinvigoration of the Agulhas Leakage in the eastern South Atlantic. However, this anomaly in the thermocline salinity was ~70% larger than the simultaneous surface anomaly, indicating that a vast amount of salty water flowed beneath the surface when the contribution of the Indian Ocean Central Water to the SACW recovered its strength, mainly between ~130 and 126 ka (Scussolini et al., 2015). Once in the subtropical gyre, the South Equatorial Current and Brazil Current would transport these salty thermocline waters to the GL-1090 region, influencing the *G. inflata* $\delta^{18}O$ signature. This process would have the same effect of cold waters generated by the North Atlantic heat piracy; that is, it would lead to a higher $\delta^{18}O$ in the thermocline. A saltier, and therefore denser thermocline in the subtropical western South Atlantic would have turned this region to an ideal source of hydrostatic instabilities for supporting the AMOC overshoot during early MIS 5e.

## 6. Conclusions

Foraminifera oxygen and carbon stable isotopes indicate that the conditions in the thermocline of the subtropical western South Atlantic were considerably distinct between the last and penultimate glacial terminations. During the TII/MIS 5e period, *G. inflata* $\delta^{18}O$ remained at high values characteristic of glacial climate for ~7 kyr, despite the onset of the Last Interglacial. This high $\delta^{18}O$ may have been produced by a cooling of ~3°C in the thermocline. Low *G. inflata* $\delta^{13}C$ and high relative abundance of *G. bulloides* corroborate the occurrence of a thicker and likely colder SACW. Such high $\delta^{18}O$ in the Santos basin thermocline suggests that this region experienced a strong emptying of its heat content during the rise of the Last Interglacial climate. Notwithstanding, the injection of salty waters due to a stronger Agulhas Leakage may also have taken part in this process, contributing for the high *G. inflata* $\delta^{18}O$ and, then, a denser thermocline. These waters may have worked as a source of hydrostatic instability, favoring the AMOC overshoot of the early Last Interglacial. Future works investigating permanent thermocline temperature (i.e., *G. inflata* Mg/Ca) will help to fully decouple the factors behind the permanence of high $\delta^{18}O$ values during a large part of the Last Interglacial in the Santos Basin.

**Acknowledgments**
We thank R. Kowsman (CENPES/Petrobras) and Petrobras Core Repository staff (Macaé/Petrobras) for providing the sediment core employed in this research. T. P. S. acknowledges the financial support from CAPES/PDSE (grant 99999.007924/2014-03). CNPq financially supported I. M. V. with a scholarship from the CsF ("Ciencia sem Fronteiras") project (grant 248819/2013-5). A. L. A. is a CNPq senior researcher (grant 306385/2013-9) and thanks them for financial support (grant 99999.002675/2015-03). C. M. C. acknowledges the financial support from FAPESP (grant 2012/17517-3), CAPES (grant 564/2015), and CNPq (grants 302607/2016-1 and 422255/2016-5). We also thank two anonymous reviewers for their constructive comments. This study was supported by the CAPES/Paleoceano project (23038.001417/2914-71). The data reported in this paper will be archived in Pangaea (www.pangaea.de).

## References

Blaauw, M., & Christeny, J. A. (2011). Flexible paleoclimate age-depth models using an autoregressive gamma process. *Bayesian Analysis*, *6*(3), 457–474. https://doi.org/10.1214/11-BA618

Böhm, E., Lippold, J., Gutjahr, M., Frank, M., Blaser, P., Antz, B., … Deininger, M. (2015). Strong and deep Atlantic meridional overturning circulation during the last glacial cycle. *Nature*, *517*(7532), 73–76. https://doi.org/10.1038/nature14059

Broecker, W. S., & Henderson, G. M. (1998). The sequence of events surrounding termination II and their implications for the causes of glacial interglacial $CO_2$ changes. *Paleoceanography*, *13*(4), 352–364. https://doi.org/10.1029/98PA00920

Broecker, W. S., & Maier-Reimer, E. (1992). The influence of air and sea exchange on the carbon isotope distribution in the sea. *Global Biogeochemical Cycles*, *6*(3), 315–320. https://doi.org/10.1029/92GB01672

Campos, M. C., Chiessi, C. M., Voigt, I., Piola, A. R., Kuhnert, H., & Mulitza, S. (2017). $\delta^{13}C$ decreases in the upper western South Atlantic during Heinrich Stadials 3 and 2. *Climate of the Past*, *13*, 345–358. https://doi.org/10.5194/cp-13-345-2017

Carlson, A. E. (2008). Why there was not a younger Dryas-like event during the Penultimate Deglaciation. *Quaternary Science Reviews*, *27*(9-10), 882–887. https://doi.org/10.1016/j.quascirev.2008.02.004

Chiessi, C. M., Mulitza, S., Paul, A., Pätzold, J., Groeneveld, J., & Wefer, G. (2008). South Atlantic interocean exchange as the trigger for the Bølling warm event. *Geology*, *36*(12), 919–922. https://doi.org/10.1130/G24979A.1

Deaney, E. L., Barker, S., & van de Flierdt, T. (2017). Timing and nature of AMOC recovery across Termination 2 and magnitude of deglacial $CO_2$ change. *Nature Communications*, *8*. https://doi.org/10.1038/ncomms14595

Garzoli, S. L., & Matano, R. (2011). The South Atlantic and the Atlantic Meridional Overturning Circulation. *Deep Sea Research Part II: Topical Studies in Oceanography*, *58*(17-18), 1837–1847. https://doi.org/10.1016/j.dsr2.2010.10.063

Gong, X., Knorr, G., Lohmann, G., & Zhang, X. (2013). Dependence of abrupt Atlantic meridional ocean circulation changes on climate background states. *Geophysical Research Letters*, *40*, 3698–3704. https://doi.org/10.1002/grl.50701

Gordon, A. L. (1981). South Atlantic thermocline ventilation. *Deep Sea Research Part A: Oceanographic Research Papers*, *28*(11), 1239–1264. https://doi.org/10.1016/0198-0149(81)90033-9

Govin, A., Chiessi, C. M., Zabel, M., Sawakuchi, A. O., Heslop, D., Hörner, T., … Mulitza, S. (2014). Terrigenous input off northern South America driven by changes in Amazonian climate and the North Brazil Current retroflection during the last 250 ka. *Climate of the Past*, *10*(2), 843–862. https://doi.org/10.5194/cp-10-843-2014

Grant, K. M., Rohling, E. J., Bar-Matthews, M., Ayalon, A., Medina-Elizalde, M., Ramsey, C. B., … Roberts, A. P. (2012). Rapid coupling between ice volume and polar temperature over the past 150,000 years. *Nature*, *491*(7426), 744–747. https://doi.org/10.1038/nature11593

Groeneveld, J., & Chiessi, C. M. (2011). Mg/Ca of Globorotalia inflata as a recorder of permanent thermocline temperatures in the South Atlantic. *Paleoceanography*, *26*, PA2203. https://doi.org/10.1029/2010PA001940

Lessa, D. V. O., Ramos, R. P., Barbosa, C. F., da Silva, A. R., Belem, A., Turcq, B., & Albuquerque, A. L. (2014). Planktonic foraminifera in the sediment of a western boundary upwelling system off Cabo Frio, Brazil. *Marine Micropaleontology*, *106*, 55–68. https://doi.org/10.1016/j.marmicro.2013.12.003

Lessa, D. V. O., Santos, T. P., Venancio, I. M., & Albuquerque, A. L. S. (2017). Offshore expansion of the Brazilian coastal upwelling zones during Marine Isotope Stage 5. *Global and Planetary Change*, *158*, 13–20. https://doi.org/10.1016/j.gloplacha.2017.09.006

Lisiecki, L. E., & Raymo, M. E. (2005). A Pliocene-Pleistocene stack of 57 globally distributed benthic $\delta^{18}O$ records. *Paleoceanography*, *20*, PA1003. https://doi.org/10.1029/2004PA001071

Lototskaya, A., & Ganssen, G. M. (1999). The structure of Termination II (penultimate deglaciation and Eemian) in the North Atlantic. *Quaternary Science Reviews*, *18*(14), 1641–1654. https://doi.org/10.1016/S0277-3791(99)00011-6

Martrat, B., Jimenez-Amat, P., Zahn, R., & Grimalt, J. O. (2014). Similarities and dissimilarities between the last two deglaciations and interglaciations in the North Atlantic region. *Quaternary Science Reviews*, *99*, 122–134. https://doi.org/10.1016/j.quascirev.2014.06.016

Masson-Delmotte, V., Stenni, B., Blunier, T., Cattani, O., Chappellaz, J., Cheng, H., … Waelbroeck, C. (2010). Abrupt change of Antarctic moisture origin at the end of Termination II. *Proceedings of the National Academy of Sciences of the United States of America*, *107*(27), 12,091–12,094. https://doi.org/10.1073/pnas.0914536107

McManus, J. F., Francois, R., Gherardi, J.-M., Keigwin, L. D., & Brown-Leger, S. (2004). Collapse and rapid resumption of Atlantic meridional circulation linked to deglacial climate changes. *Nature*, *428*(6985), 834–837. https://doi.org/10.1038/nature02494

Peeters, F. J. C., Brummer, G.-J. A., & Ganssen, G. (2002). The effect of upwelling on the distribution and stable isotope composition of *Globigerina bulloides* and *Globigerinoides ruber* (planktic foraminifera) in modern surface waters of the NW Arabian Sea. *Global and Planetary Change*, *34*(3-4), 269–291. https://doi.org/10.1016/S0921-8181(02)00120-0

Peterson, R. G., & Stramma, L. (1991). Upper-level circulation in the South Atlantic Ocean. *Progress in Oceanography*, *26*(1), 1–73. https://doi.org/10.1016/0079-6611(91)90006-8

Portilho-Ramos, R., Ferreira, F., Calado, L., Frontalini, F., & de Toledo, M. B. (2015). Variability of the upwelling system in the southeastern Brazilian margin for the last 110,000 years. *Global and Planetary Change*, *135*, 179–189. https://doi.org/10.1016/j.gloplacha.2015.11.003

Raymo, M. E. (1997). The timing of major climate terminations. *Paleoceanography*, *12*(4), 577–585. https://doi.org/10.1029/97PA01169

Richardson, P. L. (2007). Agulhas leakage into the Atlantic estimated with subsurface floats and surface drifters. *Deep Sea Research Part I: Oceanographic Research Papers*, *54*(8), 1361–1389. https://doi.org/10.1016/j.dsr.2007.04.010

Ritz, S. P., Stocker, T. F., Grimalt, J. O., Menviel, L., & Timmermann, A. (2013). Estimated strength of the Atlantic overturning circulation during the last deglaciation. *Nature Geoscience*, *6*(3), 208–212. https://doi.org/10.1038/ngeo1723

Rühlemann, C., Mulitza, S., Lohmann, G., Paul, A., Prange, M., & Wefer, G. (2004). Intermediate depth warming in the tropical Atlantic related to weakened thermohaline circulation: Combining paleoclimate data and modeling results for the last deglaciation. *Paleoceanography*, *19*, PA1025. https://doi.org/10.1029/2003PA000948

Salgueiro, E., Voelker, A., Abrantes, F., Meggers, H., Pflaumann, U., Lončarić, N., … Wefer, G. (2008). Planktonic foraminifera from modern sediments reflect upwelling patterns off Iberia: Insights from a regional transfer function. *Marine Micropaleontology*, *66*(3-4), 135–164. https://doi.org/10.1016/j.marmicro.2007.09.003

Santos, T. P., Lessa, D. O., Venancio, I. M., Chiessi, C. M., Mulitza, S., Kuhnert, H., … Albuquerque, A. L. S. (2017). Prolonged warming of the Brazil current precedes deglaciations. *Earth and Planetary Science Letters*, *463*, 1–12. https://doi.org/10.1016/j.epsl.2017.01.014

Schlitzer, R. (2003). Interactive analysis and visualization of geoscience data with ocean data view. *Computers & Geosciences*, *28*(10), 1211–1218.

Schmidt, M. W., Chang, P., Hertzberg, J. E., Them, T. R., Ji, L., & Otto-Bliesner, B. L. (2012). Impact of abrupt deglacial climate change on tropical Atlantic subsurface temperatures. *Proceedings of the National Academy of Sciences*, *109*(46), 19,034–19,034. https://doi.org/10.1073/pnas.1216897109

Schmidt, M. W., Spero, H. J., & Lea, D. W. (2004). Links between salinity variation in the Caribbean and North Atlantic thermohaline circulation. *Nature*, *428*(6979), 160–163. https://doi.org/10.1038/nature02346

Schrag, D. P., Adkins, J. F., McIntyre, K., Alexander, J. L., Hodell, D. A., Charles, C. D., & McManus, J. F. (2002). The oxygen isotopic composition of seawater during the Last Glacial Maximum. *Quaternary Science Reviews*, *21*(1–3), 331–342. https://doi.org/10.1016/S0277-3791(01)00110-X

Scussolini, P., Marino, G., Brummer, G.-J. A., & Peeters, F. J. C. (2015). Saline Indian Ocean waters invaded the South Atlantic thermocline during glacial termination II. *Geology*, *43*(2), 139–142. https://doi.org/10.1130/G36238.1

Seidov, D., & Maslin, M. (2001). Atlantic Ocean heat piracy and the bipolar climate see-saw during Heinrich and Dansgaard-Oeschger events. *Journal of Quaternary Science*, *16*(4), 321–328. https://doi.org/10.1002/jqs.595

Shackleton, N. J. (1987). Oxygen isotopes, ice volume and sea level. *Quaternary Science Reviews*, *6*(3-4), 183–190. https://doi.org/10.1016/0277-3791(87)90003-5

Stoner, J. S., Channell, J. E. T., & Hillaire-Marcel, C. (1995). Magnetic-properties of deep-sea sediments off southwest Greenland: Evidence for major differences between the last two deglaciations. *Geology*, *23*(3), 241–244. https://doi.org/10.1130/0091-7613(1995)023%3C0241

Stramma, L., & England, M. (1999). On the water masses and mean circulation of the South Atlantic Ocean. *Journal of Geophysical Research*, *104*(C9), 20,863–20,883. https://doi.org/10.1029/1999JC900139

Tedesco, K., Thunell, R., Astor, Y., & Muller-Karger, F. (2007). The oxygen isotope composition of planktonic foraminifera from the Cariaco Basin, Venezuela: Seasonal and interannual variations. *Marine Micropaleontology*, *62*(3), 180–193. https://doi.org/10.1016/j.marmicro.2006.08.002

Tomczak, M., & Godfrey, J. S. (1994). Regional oceanography: An introduction. Pergamon, Oxford. https://doi.org/10.1002/joc.3370150511

Venancio, I. M., Belem, A. L., dos Santos, T. H. R., Zucchi, M. R., Azevedo, A. E. G., Capilla, R., & Albuquerque, A. L. S. (2014). Influence of continental shelf processes in the water mass balance and productivity from stable isotope data on the Southeastern Brazilian coast. *Journal of Marine Systems*, *139*, 241–247. https://doi.org/10.1016/j.jmarsys.2014.06.009

Voigt, I., Chiessi, C. M., Prange, M., Mulitza, S., Groeneveld, J., Varma, V., & Henrich, R. (2015). Holocene shifts of the southern westerlies across the South Atlantic. *Paleoceanography*, *30*, 39–51. https://doi.org/10.1002/2014PA002677

Ziegler, M., Diz, P., Hall, I. R., & Zahn, R. (2013). Millennial-scale changes in atmospheric $CO_2$ levels linked to the Southern Ocean carbon isotope gradient and dust flux. *Nature Geoscience*, *6*(6), 457–461. https://doi.org/10.1038/ngeo1782

Zweng, M. M., Reagan, J. R., Antonov, J. I., Locarnini, R. A., Mishonov, A. V., Boyer, T. P., … Biddle, M. M. (2013). World Ocean Atlas 2013, Volume 2: Salinity. In S. Levitus, & A. Mishonov (Technical Eds.), *NOAA Atlas NESDIS* (Vol. 74, 39 pp.).